

# $\beta$ -elemene inhibits oxygen-induced retinal neovascularization via promoting miR-27a and reducing VEGF expression

WEILAI ZHANG<sup>1,2</sup>, LEI CHEN<sup>1</sup>, JIN GENG<sup>1</sup>, LIMIN LIU<sup>1</sup> and LI XU<sup>2</sup><sup>1</sup>Department of Ophthalmology, The First Affiliated Hospital of China Medical University, Shenyang, Liaoning 110001;<sup>2</sup>Department of Ophthalmology, The Fourth People's Hospital of Shenyang, Shenyang, Liaoning 110031, P.R. China

Received May 17, 2018; Accepted December 14, 2018

DOI: 10.3892/mmr.2019.9863

**Abstract.** The present study aimed to investigate the significant role of  $\beta$ -elemene in mouse models of oxygen-induced retinopathy (OIR). C57BL/6J neonatal mice were used to establish OIR models. They were divided into four groups: Normoxia, OIR, OIR control and OIR-treated. Mice in the OIR group were exposed to  $75\pm 5\%$  oxygen for 5 days and returned to a normal oxygen environment on postnatal day 12 (P12). The OIR treated group was intravitreally injected with  $1\ \mu\text{l}$   $\beta$ -elemene on P12 and subsequently returned to a normal oxygen environment for 5 days (P12-P17). Retinas were obtained on P17. Retinal neovascularization (RNV) was detected using adenosine diphosphatase staining and analyzed by counting the nuclei of neovascular endothelial cells. Vascular endothelial growth factor (VEGF) expression was determined by reverse transcription-quantitative polymerase chain reaction, immunohistochemistry and western blot analysis. MicroRNA (miRNA/miR) microarrays were used to screen out differentially expressed miRNAs between the OIR and  $\beta$ -elemene-treated groups. Binding the 3'-untranslated region (UTR) of VEGF and miR-27a was confirmed using luciferase assays. It was found that high oxygen concentrations accelerated RNV and increased the number of preretinal neovascular cells;  $\beta$ -elemene treatment reduced these effects. VEGF mRNA and protein expression was higher in the OIR and OIR control groups, compared with the normoxia and OIR-treated groups. Further, it was shown that miR-22, miR-181a-1, miR-335-5p, miR-669n, miR-190b, miR-27a and miR-93 were upregulated in the OIR-treated group, and downregulated in the OIR group. The prediction websites TargetScan and miRanda revealed that VEGF contained a potential miR-27a binding site in its 3'-untranslated region (UTR). Luciferase assays demonstrated that miR-27a directly

bound to the 3'-UTR of VEGF. *In vitro* experiments demonstrated that miR-27a inhibited VEGF expression. In addition,  $\beta$ -elemene treatment upregulate miR-27a expression *in vivo* and *in vitro*. When miR-27a expression was depleted by miR-27a inhibitor, the protective effect of  $\beta$ -elemene on RNV was eliminated. The present study demonstrated that  $\beta$ -elemene reduced RNV in mouse OIR models via miR-27a upregulation, leading to reduced VEGF expression. This finding may contribute to the development of novel therapeutic strategies for human retinopathy.

## Introduction

Intraocular neovascularization is an important clinical manifestation which is the pathological basis for numerous ocular disorders, such as proliferative diabetic retinopathy, ischemic central retinal vein occlusion and retinopathy of prematurity (1-3). No effective treatment for retinal neovascularization (RNV) is available to date. Recent studies have shown that retinal angiogenesis may due to complex interactions among multiple angiogenic stimulators (4,5).

$\beta$ -elemene, isolated from the Chinese medicinal herb Zedoary (*Curcuma zedoaria*) exhibits substantial clinical activity against various cancers *in vitro* and *in vivo* (6-8).  $\beta$ -elemene reduces the proliferation of blood vessel endothelial cells during tumor progression by inhibiting the expression of angiogenic factors, such as vascular endothelial growth factor (VEGF) and Notch-1 (9,10). The previously reported effects of  $\beta$ -elemene in vascularization prompted us to examine the therapeutic effects of  $\beta$ -elemene on RNV. The present study investigated the suppressive effects of  $\beta$ -elemene on RNV in a mouse model of oxygen-induced retinopathy (OIR). The results showed that  $\beta$ -elemene inhibited RNV in OIR mice and downregulated the expression of VEGF in the retina.

It is well known that VEGF is an important factor that stimulates endothelial cell proliferation and tube formation, and also mediates oxygen-induced RNV (11,12). Therefore, understanding the abnormal regulation of VEGF may contribute to the identification of effective RNV therapies. In order to elucidate the underlying mechanisms of  $\beta$ -elemene-mediated inhibition of VEGF expression, the present research focused on microRNAs (miRNAs/miRs). Previous studies have shown a series of miRNAs, including miR-9, miR-410 and miR-146a, inhibit retinal neovascularization by targeting VEGF (13-15).

*Correspondence to:* Dr Lei Chen, Department of Ophthalmology, The First Affiliated Hospital of China Medical University, 155 Nanjingbei Street, Shenyang, Liaoning 110001, P.R. China  
E-mail: 18660232387@163.com

**Key words:**  $\beta$ -elemene, microRNA-27a, retinal neovascularization, vascular endothelial growth factor

In the present study, miRNA microarrays were used to screen the miRNAs with different expression levels between the OIR and  $\beta$ -elemene-treated groups. Prediction websites TargetScan and miRanda, as well as luciferase assays, were used to demonstrate that miR-27a directly bound to the 3'-untranslated region (UTR) of VEGF and inhibited its expression, suggesting that VEGF was a direct target of miR-27a. In addition, it was demonstrated that  $\beta$ -elemene upregulated miR-27a expression *in vivo* and *in vitro*. Furthermore, miR-27a inhibitor transfection eliminated the effects of  $\beta$ -elemene on RNV, suggesting that  $\beta$ -elemene reduced RNV via miR-27a.

Taken together, it was concluded that  $\beta$ -elemene inhibited RNV in OIR mouse models, by reducing VEGF expression via miR-27a upregulation. This novel finding may encourage further exploration of the role of  $\beta$ -elemene in the pathogenesis of these diseases.

## Materials and methods

**Animals.** Animal experiments were conducted following the guidelines of the Animal Experiment Committee of The First Affiliated Hospital of China Medical University, and the study was approved by the ethics committee of The First Affiliated Hospital of China Medical University (Shenyang, China). Mice were maintained in a 12 h light/dark cycle at 23–25°C with 50–60% humidity. C57BL/6J neonatal mice (23–28 g; routinely fed water and food) were used to establish OIR models on post-natal day 7 (P7), according to the Smith's method (16). A total of 80 mice (37 male and 43 female) were randomly divided into 4 groups: i) Normoxia; ii) OIR; iii) OIR control; and iv) OIR treated. Mice in the normoxia group were maintained under normoxic conditions (oxygen concentration, 15±2%) for 17 days. The mice in the OIR group were exposed to 75±5% oxygen for 5 days and returned to a normal oxygen environment on P12. The OIR control and OIR treated groups were intravitreally injected with 1  $\mu$ l lipid emulsion (0.25 mg/ml; Dalian Yuanda Pharmaceutical Co., Ltd., Dalian, China) and  $\beta$ -elemene (0.25 mg/ml, Dalian Yuanda Pharmaceutical Co., Ltd.), respectively, on P12 and subsequently returned to a normal oxygen environment for 5 days (P12–P17). Rats were anesthetized with chloral hydrate (430 mg/kg; 4.3%) prior to intravitreal injection.

**Observation of RNV.** On P17, all mice were sacrificed and the eyes were harvested. The cornea, lens and vitreous humor were removed, and the retinas were surgically dissected. The retinas were fixed with 4% paraformaldehyde for 8 h at 37°C, and retinal sections (1 mm) were prepared for adenosine diphosphatase (ADPase) staining (10% ammonium sulfide) and flat-mounted on microscope slides with a gelatin-coated coverslip. Each retina was divided into 12 equal segments and observed under an optical microscope (x200; Olympus Corporation, Tokyo, Japan) and the proportion of neovascularization areas were counted, as described previously (17). Three independent reviewers were blinded to grouping to assess the severity of RNV.

**Quantification of RNV.** The mice were sacrificed, and the eyes were enucleated, immersed in 40 g/l paraformaldehyde in PBS for at least 24 h at 37°C and embedded in paraffin. Serial 6- $\mu$ m sections from all eyes were cut sagittally, parallel to the

optic nerve and stained with hematoxylin and eosin (H&E) for 3 min at 37°C. The preretinal neovascular cell nuclei, identified under a light microscope (x200), were considered to be associated with new vessels if they were found on the vitreal side of the internal limiting membrane (ILM) (18). The preretinal neovascular cells were counted to quantitatively assess RNV (11,19). All retinas were examined in five serial sections. Three independent reviewers were blinded to grouping when counting the cells.

**RNA preparation and reverse transcription-quantitative polymerase chain reaction (RT-qPCR).** Total RNA was extracted from retinal tissues by TRIzol reagent (Invitrogen; Thermo Fisher Scientific, Inc., Waltham, MA, USA) following the manufacturer's protocol. RT-qPCR was performed using SYBR Premix Ex Taq (Takara Bio, Inc., Otsu, Japan) on a Thermal Cycler Dice™ Real Time system (Takara Bio, Inc.) using the following thermocycling conditions: 30 sec at 95°C followed by two-step PCR for 40 cycles of 95°C for 5 sec and 64°C for 30 sec. The primer sequences were as follows: VEGF forward, 5'-CAACTTCTGGGCTCTTCTCG-3'; VEGF reverse, 5'-CCTCTCCTTCTCTTCTCTTCC-3'; miR-27a forward, 5'-CAACTTCTGGGCTCTTCTCG-3'; miR-27a reverse, 5'-GTCAGCGGACTCTGGATTGAG-3'; GAPDH forward, 5'-ATAGCACAGCCTGGATAGCAACGTAC-3'; GAPDH reverse, 5'-CACCTTCTACAATGAGCTGCGTGTG-3'; U6B forward, 5'-CTCGCTTCGGCAGCACATATACT-3'; U6B reverse, 5'-ACGCTTACGAATTTGCGTGTG-3'. GAPDH was used as a reference control of VEGF. U6B was used as a reference control of miR-27a. All primers were purchased from Sangon Biotech Co., Ltd. (Shanghai, China). Relative gene expression data was analyzed using the  $2^{-\Delta\Delta C_q}$  method (20).

**Immunohistochemistry (IHC).** Retinas were fixed in 4% paraformaldehyde for 48 h at 37°C, embedded in paraffin and cut into 4- $\mu$ m sections. Following general deparaffinization, antigen retrieval was performed for 1 min with an autoclave using 0.01 mol/l sodium citrate buffer. H<sub>2</sub>O<sub>2</sub> (0.3%) was used to block endogenous peroxidase activity. Goat serum (6%; Maixin-Bio, Fuzhou, China) was used to block the nonspecific immunoglobulin-binding sites for 20 min at 37°C. The slices were incubated overnight with anti-VEGF (1:200; cat. no. 1402390; Sigma-Aldrich, MO, USA) at 4°C, rinsed with PBS and incubated with goat anti-rabbit immunoglobulin G secondary antibody (1:200; Sigma-Aldrich; Merck KGaA, Darmstadt, Germany) for 30 min at 37°C. The peroxidase reaction was developed with 3,3'-diaminobenzidine tetrahydrochloride (DAB). The sections were counterstained with Mayer's hematoxylin for 1 min at 37°C, dehydrated, cleared in xylene and mounted in Permount medium (Thermo Fisher Scientific, Inc.).

**In situ hybridization (ISH).** The ISH kit was purchased from Wuhan Boster Biological Technology, Ltd. (Wuhan, China) and used according to the manufacturer's protocol. In brief, tissue slides were hybridized with 20  $\mu$ l 5-digoxigenin LNA-modified-miR-27a-3p (synthesized by Wuhan Boster Biological Technology, Ltd.). The sequence was 5'-TTCAGC CCCATGTTTGCCCTC-3'. The peroxidase reaction was developed with DAB.

**Quantitative assessment and scoring.** The expression of VEGF and miR-27a detected in the immunohistochemical and ISH analysis was quantitatively assessed using Image-Pro Plus Software 6.0 (Media Cybernetics, Inc., Rockville, MD, USA). The integrated optical density of retina sections was calculated by two investigators in a double blinded manner.

**Western blot analysis.** A total protein extraction kit (Beijing Solarbio Science & Technology, Co., Ltd., Beijing, China) was used to extract protein according to the instructions. Ultraviolet absorption was the protein determination method. Proteins (40  $\mu\text{g}/\text{lane}$ ) were separated by 10% SDS-PAGE and transferred onto polyvinylidene difluoride membranes. Next, 5% skimmed milk solution in Tris-buffered saline with Tween 20 (0.05%) buffer was used to block the membranes, which were then incubated with VEGF (1:2,000; cat. no. 1402390; Sigma-Aldrich; Merck KGaA), platelet-derived endothelial cell growth factor (PD-ECGF; 1:2,000; Abcam; Cambridge, UK), transforming growth factor  $\beta$  (TGF- $\beta$ ; cat. no. ab186838; 1:1,500; Abcam), tumor necrosis factor  $\alpha$  (TNF- $\alpha$ ; cat. no. ab6671; 1:2,000; Abcam) and GADPH (cat. no. 60004-1-Ig; 1:2,000; ProteinTech Group, Inc. Chicago, IL, USA), antibodies overnight at 4°C. Next, membranes were incubated with goat anti-rabbit IgG secondary antibody (cat. no. TA130015; OriGene Technologies, Inc., Beijing, China) for 2 h at room temperature. Proteins were visualized using an enhanced chemiluminescence system (Merck KGaA).

**miRNA PCR array.** Total RNA was extracted from the retinal tissues of the normoxia, OIR, and OIR-treated groups using TRIzol<sup>®</sup> reagent (Invitrogen; Thermo Fisher Scientific, Inc.) and cleaned with the RNeasy\_MinElute Cleanup kit (Qiagen GmbH, Hilden, Germany). SuperScript III Reverse Transcriptase (Qiagen GmbH) was used to reverse transcribe the total RNA, and cDNA was amplified by polymerase chain reaction using the 2\_Super Array PCR Master mix (Qiagen GmbH). The MicroRNA PCR array (SuperArray Bioscience Corporation, Frederick, MD, USA) was performed in a Thermal Cycler Dice Real-Time system (Takara Bio, Inc.) according to the manufacturer's protocol. The results were normalized to U6B levels using the 2<sup>- $\Delta\Delta\text{C}_q$</sup>  method (21).

**Luciferase assays.** Cells (293T, Procell Life Technology Co., Ltd., Wuhan, China) were plated into 24-well plates at 80% confluence 24 h before transfection. The wild-type VEGF-3'UTR (WT) and mutant VEGF-3'UTR (MUT) containing the binding site of miR-27a-3p were established and cloned into a Firefly luciferase-expressing vector (Obio Technology Corp., Ltd., Shanghai, China). A mixture of 200 ng WT or MUT, 700 ng pGV214-miR-27a and 100 ng *Renilla* luciferase plasmid were transfected into 293T cells using Lipofectamine<sup>®</sup> 2000. A dual-luciferase reporter system (Promega Corporation, Madison, WI, USA) was used to evaluate Firefly and *Renilla* luciferase activity 36 h after transfection.

**In vitro cell culture.** Mouse retinal microvascular endothelial cells (cat. no. CM-2098) were obtained from Cmbio company (Shanghai, China, [www.biomart.cn/infosupply/63235021.htm](http://www.biomart.cn/infosupply/63235021.htm)). The cells were cultured in Endothelial Cell Medium

(Beijing Solarbio Science & Technology, Co., Ltd.) with 10% fetal bovine serum (Absin Bioscience, Inc., Shanghai, China) and 100 units/ml of penicillin and streptomycin (Hyclone; GE Healthcare Life Sciences, Logan, UT, USA) in an incubator with 5% CO<sub>2</sub> at 37°C. Cells in passage two were used for subsequent experiments.

**Oligonucleotide transfection.** miR-27a mimic, inhibitor and miR-27a control oligonucleotides were purchased from Shanghai GenePharma Co., Ltd. (Shanghai, China). Transfection was performed using Lipofectamine<sup>®</sup> 2000 (Invitrogen; Thermo Fisher Scientific, Inc.) according to the manufacturer's protocol. The oligonucleotide sequences were as follows: miR-27a mimic, sense 5'-UAACUACAUGGU UAACCUCUUU-3' and antisense 5'-AGAGGUUAACCA UGUUAUGUAA-3'; miR-27a inhibitor, sense 5'-AGGGCT TAGCTGCTTGTGAGCA-3' and antisense 5'-TTCACAGTG GCTAAGTCCGC-3'; negative control, sense 5'-AACUCC GAACGUGUCACGUGT-3' and antisense 5'-AUGUGACAC GUUCGGAGAAGT-3'. Mice in the OIR treated group were administered injections of 1  $\mu\text{l}$  miR-27a inhibitor or miR-27a control with a 33-gauge needle attached to a Hamilton syringe on P11. On P12, mice were injected with 1  $\mu\text{l}$   $\beta$ -elemene, and subsequently returned to a normal oxygen environment for 6 days (P12-P17).

**Cell Counting Kit-8 (CCK-8) assay.** Treated cells (2,000/well) were plated in a 96-well plate and incubated for 24, 48, 72 and 96 h. Following each time point, 10  $\mu\text{l}$  CCK8 solution (Beijing Solarbio Science & Technology, Co., Ltd.) was added to each well and incubated for additional 1 h at 37°C. The results were quantified spectrophotometrically at a wavelength of 450 nm.

**Statistical analysis.** SPSS version 17.0 (SPSS, Inc., Chicago, IL, USA) was applied to complete data processing. All data were presented as the mean  $\pm$  standard deviation. Statistical significance was evaluated by one-way analysis of variance with the Least Significant Difference test for post-hoc analysis.  $P < 0.05$  was considered to indicate a statistically significant difference.

## Results

**Quantification of RNV.** The results of H&E-stained retinal sections showed an average of  $3.11 \pm 2.03$  nuclei per cross-section in the normoxia group (Fig. 1A), compared with  $23.11 \pm 6.75$  and  $21.67 \pm 8.5$  in the OIR (Fig. 1B) and OIR control (Fig. 1C) groups, respectively ( $P < 0.05$ ). Furthermore, the average number of preretinal neovascular cells in the OIR-treated group ( $5.89 \pm 2.03$ ; Fig. 1D) decreased significantly compared with the OIR and OIR control groups ( $P < 0.05$ ), confirming the anti-neovascularization effects of  $\beta$ -elemene on RNV (Fig. 1E).

**Qualitative analysis of RNV.** Retinal vasculature was examined in the normoxia, OIR, OIR control, and OIR treated groups by ADPase staining in retinal flat mounts at P17. No abnormal blood vessels were observed in the retinas of the normoxia group (Fig. 2A). Two layers of retinal vessels were evenly distributed in the retina, the superficial blood vessels were well formed, and the deep blood vessel formed a

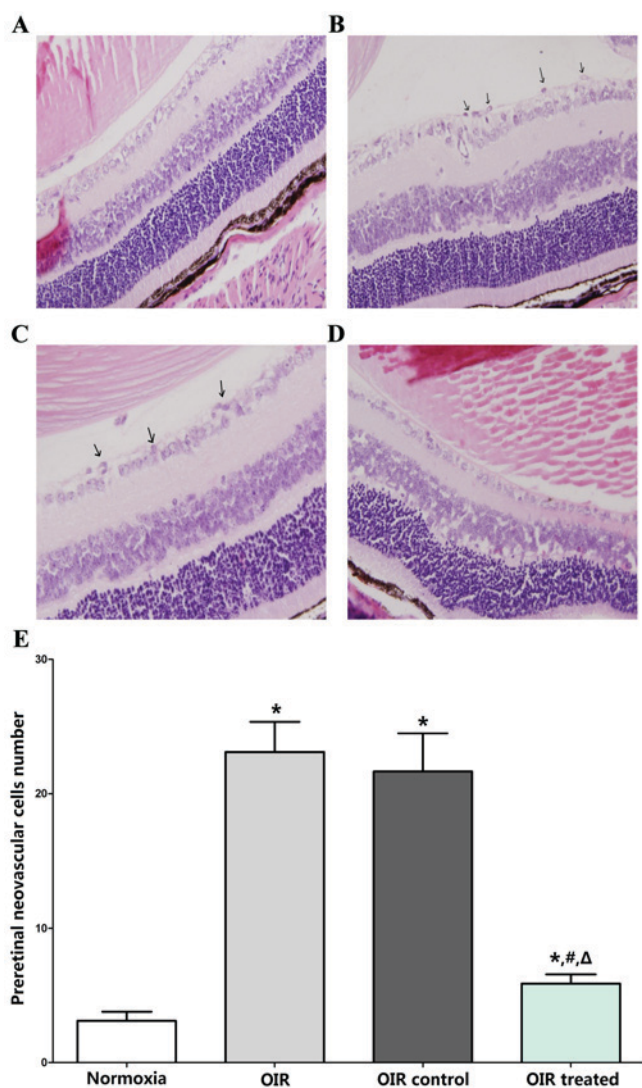


Figure 1. Preretinal neovascular cells were counted in four groups. (A-D) Images shown are of representative retinal sections from the (A) normoxia, (B) OIR, (C) OIR control and (D) OIR treated groups. The black arrows indicate preretinal neovascular cells (magnification,  $\times 400$ ). (E) Statistical analysis of preretinal neovascular cell number. Three independent reviewers were blinded to grouping when counting the cells. Data are shown as the mean  $\pm$  standard deviation. \* $P < 0.05$  vs. normoxia group, # $P < 0.05$  vs. OIR group, and  $\Delta P < 0.05$  vs. OIR control group. OIR, oxygen-induced retinopathy.

polygon mesh pattern. The blood vessels in OIR (Fig. 2B) and OIR control groups (Fig. 2C) showed non-perfusion areas and neovascularization. The ratio of new blood vessel area to total retinal area was higher in the OIR treated ( $23 \pm 6\%$ ), OIR ( $56 \pm 8\%$ ), and OIR control groups ( $47 \pm 10\%$ ) than in the normoxia group ( $12 \pm 4\%$ ; all  $P < 0.05$ ; Fig. 2D and E). By contrast, retinas in the OIR treated group ( $23 \pm 6\%$ ) developed less severe neovascular tufts and regions of non-perfusion, compared with the OIR ( $56 \pm 8\%$ ,  $P < 0.05$ ) and OIR control groups ( $47 \pm 10\%$ ,  $P < 0.05$ ), which demonstrated a strong inhibitory effect of  $\beta$ -elemene on RNV in the OIR treated group. No significant difference was detected between the OIR and OIR control groups ( $P > 0.05$ ).

*$\beta$ -elemene inhibits VEGF expression.* The results of RT-qPCR and western blot analysis showed that the expression levels of

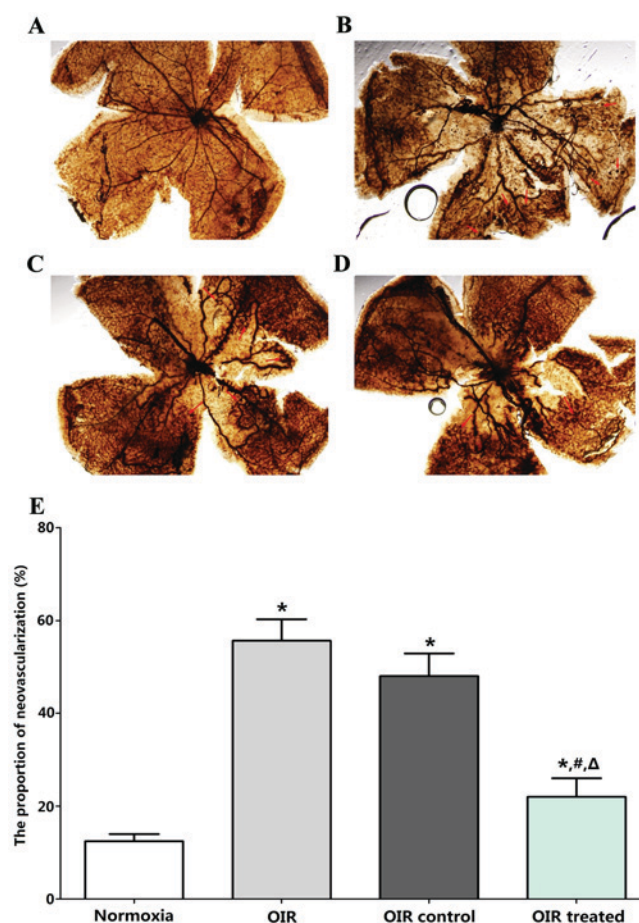


Figure 2. Adenosine diphosphatase staining of retinas. (A-D) The images are representative retinal angiographs from the eyes of the (A) normoxia, (B) OIR, (C) OIR control and (D) OIR treated groups. The red arrows indicate neovascularization (magnification,  $\times 40$ ). (E) Statistical analysis of the proportion of neovascularization. Three independent reviewers were blinded to grouping when counting the proportion of neovascularization areas in order to assess severity of retinal neovascularization. Data are presented as the mean  $\pm$  standard deviation. \* $P < 0.05$  vs. normoxia group, # $P < 0.05$  vs. OIR group, and  $\Delta P < 0.05$  vs. OIR control group. OIR, oxygen-induced retinopathy.

VEGF mRNA and protein in the normoxia and OIR treated groups were low, compared with the OIR and OIR control groups (Fig. 3A and B). Consistently, the IHC results showed that VEGF expression was higher in the OIR and OIR control groups, compared with the normoxia and OIR-treated groups (Fig. 3C-G). In addition, the effect of  $\beta$ -elemene treatment on the expression of other angiogenic factors, including PD-ECGF, TGF and TNF was detected, and it was found that  $\beta$ -elemene had no effect (data not shown). The aforementioned experimental results indicated that high oxygen concentration upregulated VEGF expression to promote retinal angiogenesis, and  $\beta$ -elemene suppressed this effect.

*miRNA microarray analysis.* miRNA microarrays were used to screen out differentially expressed miRNAs between the OIR and  $\beta$ -elemene-treated groups, in order to examine the mechanisms underlying the inhibitory effect of  $\beta$ -elemene on VEGF expression to reduce RNV (Fig. 4A). The results showed that the following miRNAs were upregulated in the OIR-treated group and downregulated in the OIR group (Fig. 4B): miR-22 (3.17-fold), miR-181a-1 (21.36-fold), miR-335-5p (3.60-fold),

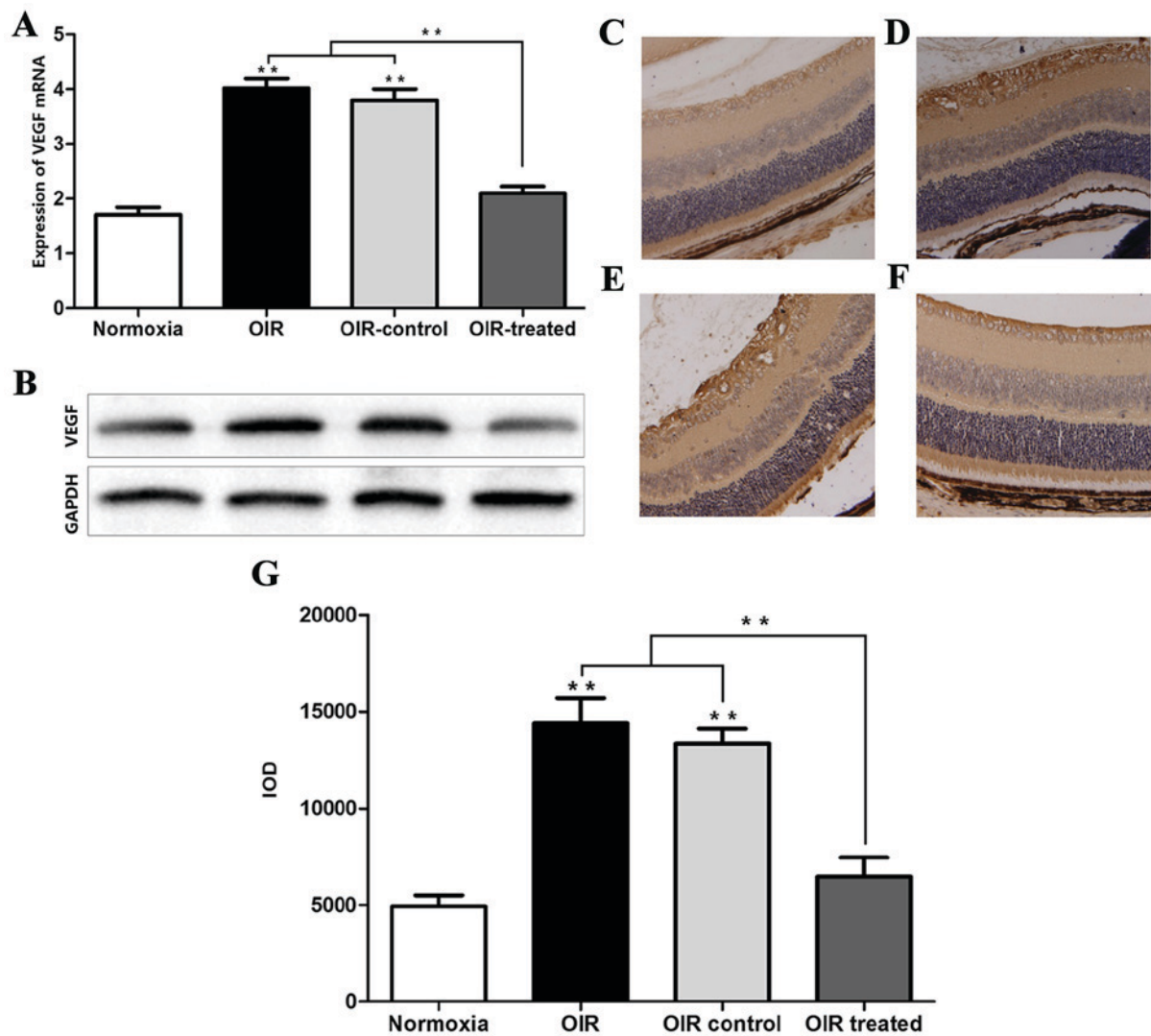


Figure 3. VEGF mRNA and protein expression is decreased by  $\beta$ -elemene treatment. (A) VEGF mRNA expression was detected by reverse transcription-quantitative polymerase chain reaction. (B) VEGF protein expression was determined by western blotting. (C-F) VEGF expression and localization was determined by IHC analysis in the (C) normoxia, (D) OIR, (E) OIR control and (F) OIR treated groups. (G) IHC analysis of VEGF expression was quantified by determining the IOD value with Image-Pro Plus software. The IOD in OIR and OIR control groups was high, compared with the normoxia and OIR treated groups ( $^{**}P<0.01$ ). There was no statistical difference between normoxia and OIR treated group ( $P>0.05$ ). IOD, integrated optical density; IHC, immunohistochemistry; VEGF, vascular endothelial growth factor; OIR, oxygen-induced retinopathy.

miR-669n (2.99-fold), miR-190b (3.68-fold), miR-27a (3.99-fold), and miR-93 (3.31-fold).

*VEGF is a target gene of miR-27a.* The potential target genes of the above miRNAs were detected according to prediction websites TargetScan and miRanda. The 3'-UTR of VEGF was found to contain one potential miR-27a-binding site (Fig. 4C). Next, luciferase assays were performed to test whether miR-27a directly bound to VEGF. The vectors containing the wild-type and mutant 3'-UTR of VEGF fused downstream of the Firefly luciferase gene are shown in Fig. 5A. The results indicated that miR-27a decreased the relative luciferase activity of the wild-type VEGF 3'-UTR (45%), compared with the mutant 3'-UTR (Fig. 5B), suggesting that VEGF may be one of the target genes of miR-27a. miR-27a mimics were subsequently transfected into mouse retinal microvascular endothelial cells to upregulate miR-27a expression (Fig. 5C). The results showed overexpression of miR-27a decreased the expression of VEGF

at both the mRNA and protein level ( $P<0.05$ ; Fig. 5D). Taken together, these results confirmed that VEGF was a direct target of miR-27a.

*$\beta$ -elemene promotes miR-27a expression.* RT-qPCR showed that the miR-27a expression in the normoxia, OIR, and OIR control groups was low, compared with the OIR-treated group (Fig. 6A). Consistent with the miR-27a expression trends in RT-qPCR, ISH experiments showed that miR-27a was predominantly expressed in retinal endothelial cells and was higher in the OIR-treated group, compared with the normoxia, OIR and OIR control groups (Fig. 6B-F). These results indicated that  $\beta$ -elemene promoted miR-27a expression. In the *in vitro* experiments, mouse retinal microvascular endothelial cells were treated with different concentrations of  $\beta$ -elemene. The results showed that  $\beta$ -elemene promoted miR-27a expression at concentrations exceeding 50  $\mu$ g/ml (Fig. 7A).

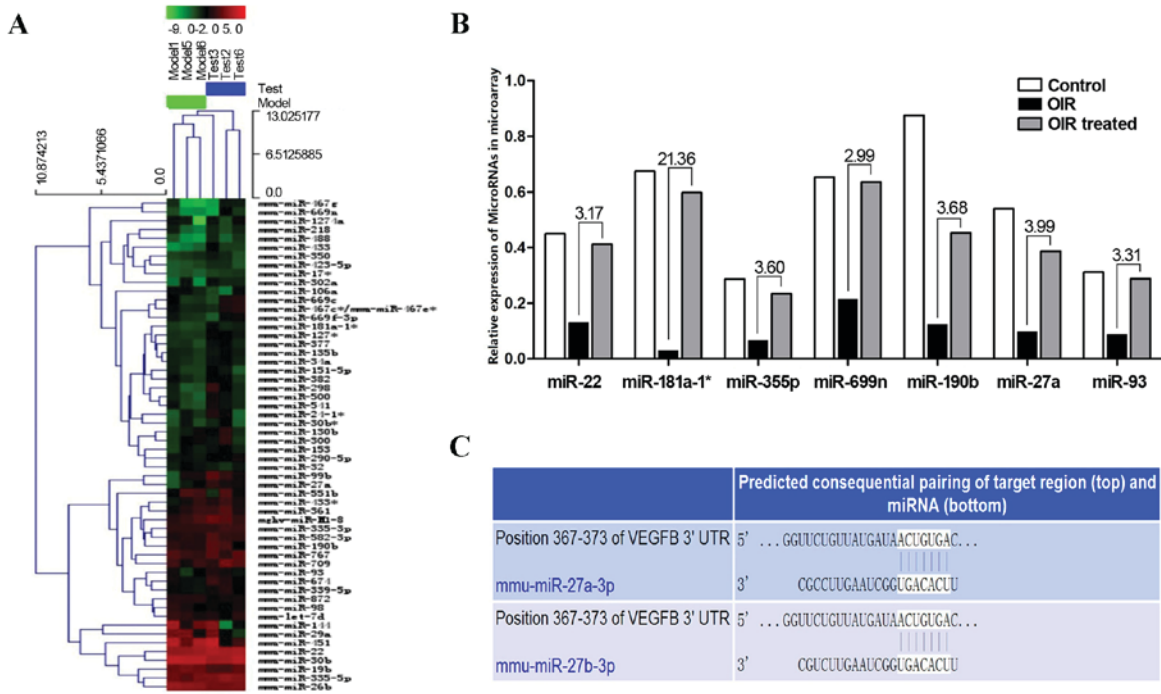


Figure 4. Differentially expressed miRNAs in the OIR and OIR treated groups. (A) Heat map of the miRNA microarray. (B) miR-22, miR-181a-1, miR-335-5p, miR-669n, miR-190b, miR-27a, miR-93 were upregulated in the OIR treated group and downregulated in the OIR group. The numbers above the histogram indicate the ratio of miRNA expression (OIR treated:OIR). (C) TargetScan and miRanda predicted that VEGF contained one potential miR-27a binding site in its 3'-UTR. miRNA/miR, microRNA; OIR, oxygen-induced retinopathy; VEGF, vascular endothelial growth factor; UTR, untranslated region.

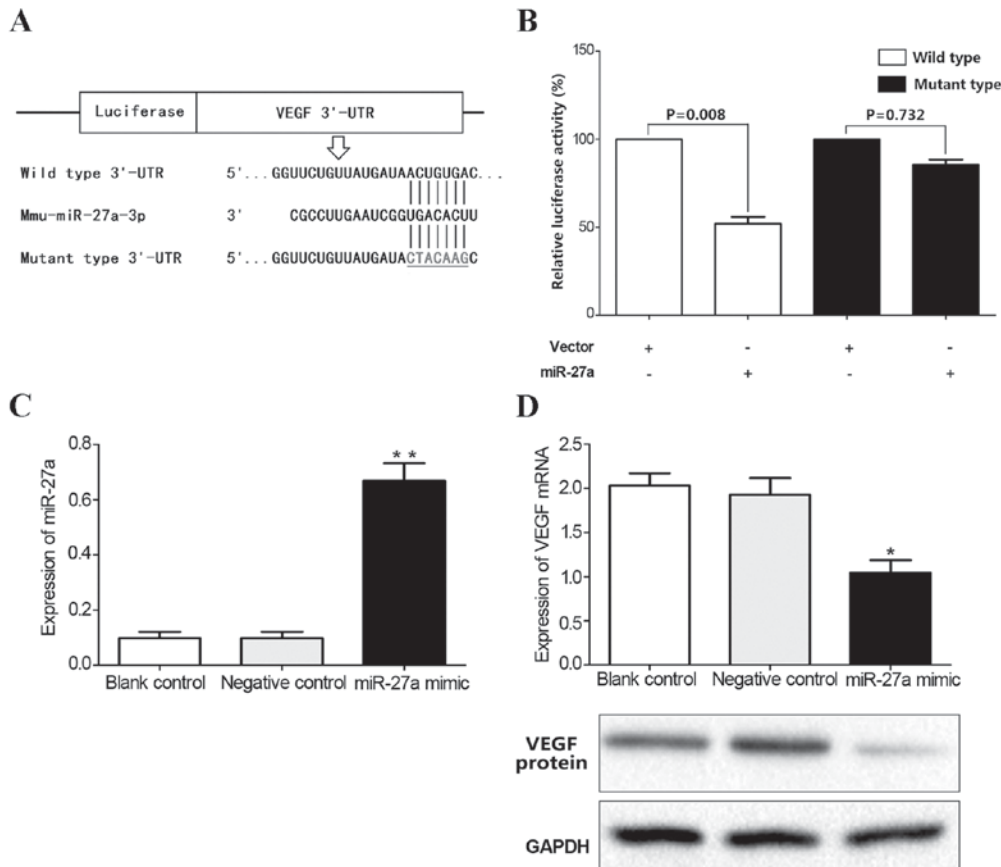


Figure 5. Luciferase assays demonstrated that miR-27a directly binds to the 3'-UTR of VEGF. (A) Wild-type and miR-27a binding site-mutated 3'-UTRs of VEGF. Mutations are underlined. (B) miR-27a significantly decreased the relative luciferase activity of the wild-type VEGF 3'-UTR (45%), compared with the mutant 3'-UTR. (C) miR-27a mimic transfection into mouse retinal microvascular endothelial cells successfully upregulated miR-27a expression. \*\*P<0.01 vs. Blank control or Negative control. (D) Overexpression of miR-27a decreased the expression of VEGF at both the mRNA and protein levels. \*P<0.05, \*\*P<0.01 vs. blank or negative control. miR, microRNA; VEGF, vascular endothelial growth factor; UTR, untranslated region.

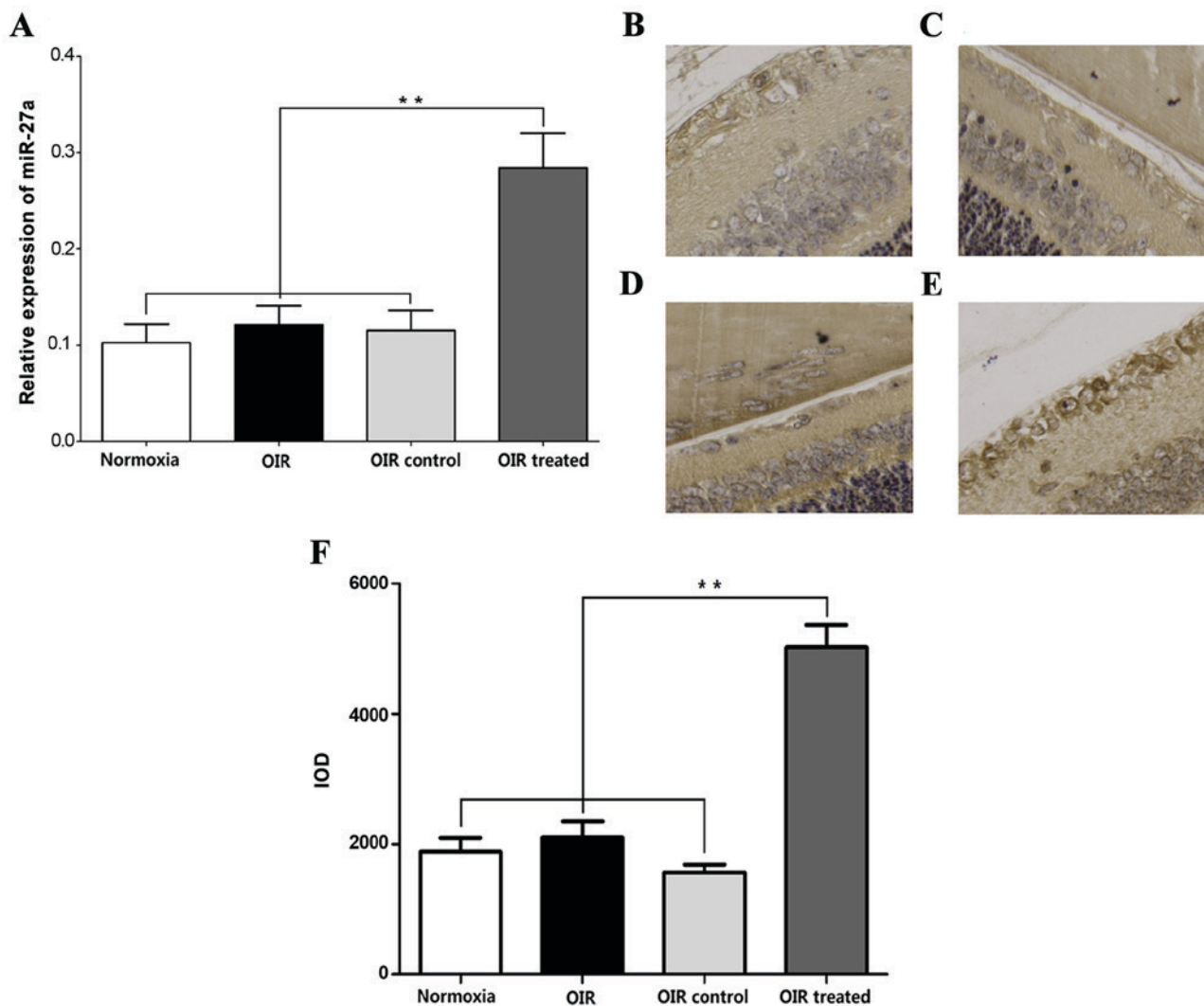


Figure 6.  $\beta$ -elemene treatment increases miR-27a expression. (A) miR-27a expression was measured by reverse transcription-quantitative polymerase chain reaction. (B-E) ISH showed miR-27a expression and localization in the (B) normoxia, (C) OIR, (D) OIR control and (E) OIR treated groups. (F) The expression of miR-27a, as determined by ISH, was quantified by measuring the IOD value with Image-Pro Plus. There was no statistical difference between normoxia, OIR and OIR control groups ( $P>0.05$ ). \*\* $P<0.01$ . miR, microRNA; ISH, *in situ* hybridization; IOD, integrated optical density; OIR, oxygen-induced retinopathy.

*$\beta$ -elemene reduces RNV via miR-27a in vivo.* The successful downregulation of miR-27a expression by its inhibitor was confirmed in normoxia (Fig. 7B) and OIR conditions *in vivo* (Fig. 7C). *In vitro*, CCK-8 assays showed that  $\beta$ -elemene inhibited cellular proliferation, and miR-27a depletion eliminated  $\beta$ -elemene's efficacy (Fig. 7D). For the *in vivo* experiments, miR-27a inhibitor was injected into the retina to reduce miR-27a expression. The retinas were dissected and processed for H&E and ADPase staining to assess RNV. H&E staining revealed an average of  $21.42\pm 3.03$  nuclei per cross-section in the OIR treated + miR-27a inhibitor group, compared with  $5.89\pm 2.03$  and  $6.89\pm 3.66$  in the OIR treated and OIR treated + miR-27a control groups, respectively ( $P<0.05$ ; Fig. 7E). According to the ADPase staining results (Fig. 7F), the ratio of new blood vessel area to total retinal area was higher in the OIR treated + miR-27a inhibitor group ( $53\pm 10\%$ ), compared with the OIR treated ( $28\pm 8\%$ ,  $P<0.05$ ) and OIR treated + miR-27a control group ( $26\pm 7\%$ ;  $P<0.05$ ). These results indicated that depletion of miR-27a expression eliminated the protective effects of  $\beta$ -elemene on oxygen-induced RNV.

## Discussion

RNV is a key process in several types of proliferative ischemic retinopathies (22,23). It is stimulated by one or more angiogenic factors released by the retina under ischemic or hypoxic conditions (24). VEGF has been demonstrated to be a major pathogenic factor and therapeutic target in retinal angiogenic diseases (11,12). It stimulates endothelial cell proliferation and tube formation and mediates ischemia-induced RNV (25,26). Previous studies have demonstrated that intravitreal injection of anti-VEGF antibody (such as bevacizumab or ranibizumab) is effective. However, neither of these drugs provide sensitive and specific effects on RNV (2,27). Therefore, finding a more effective method to suppress VEGF expression to restrain RNV has become a research hotspot.

The present study showed that  $\beta$ -elemene, a prominent component of traditional Chinese medicines, reduced the progression of RNV in a mouse model of OIR. Furthermore, the results of RT-qPCR, western blotting and IHC analyses

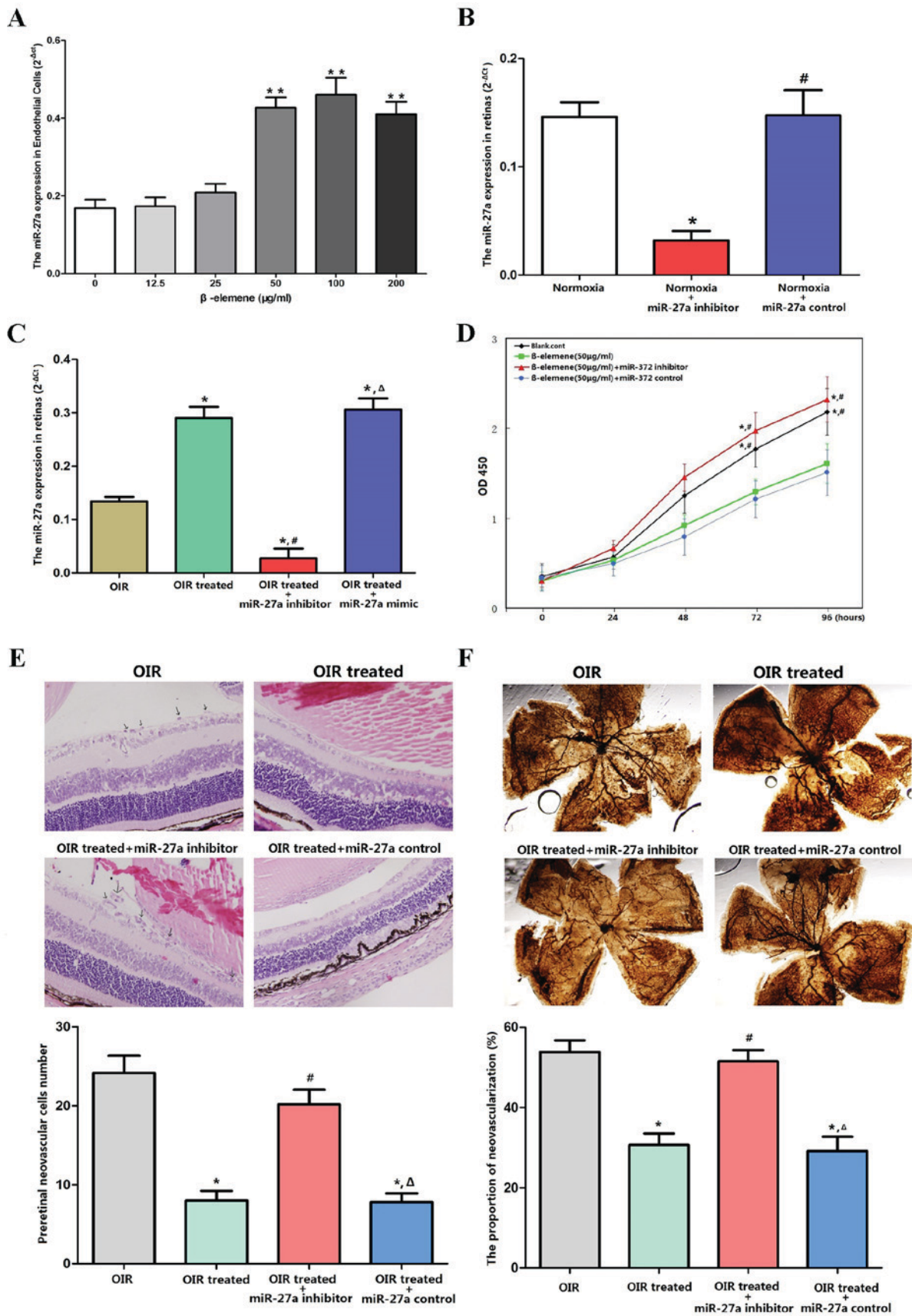


Figure 7.  $\beta$ -elemene reduces RNV via miR-27a. (A) Mouse retinal microvascular endothelial cells were treated with different concentrations of  $\beta$ -elemene. miR-27a expression was increased with concentrations of  $\beta$ -elemene above 50  $\mu\text{g/ml}$ . \*\* $P < 0.01$  vs. 0  $\mu\text{g/ml}$  group. (B and C) miR-27a inhibitor significantly decreased miR-27a expression in (B) normoxia and (C) OIR conditions. (D) Mouse retinal microvascular endothelial cell proliferation was detected by Cell Counting Kit-8 assays \* $P < 0.05$  vs.  $\beta$ -elemene group; # $P < 0.05$  vs.  $\beta$ -elemene+miR-27a control group. (E and F) miR-27a inhibitor was injected into the retina to reduce miR-27a expression. The retinas were dissected and processed for (E) hematoxylin and eosin staining, as well as (F) adenosine diphosphatase staining to assess RNV. \* $P < 0.05$  vs. OIR group; # $P < 0.05$  vs. OIR treated group;  $\Delta P < 0.05$  vs. OIR treated+miR-27a inhibitor group. miR, microRNA; OIR, oxygen-induced retinopathy; OD, optical density.



indicated that high-oxygen conditions upregulated VEGF expression.  $\beta$ -elemene suppressed this effect and down-regulated VEGF expression. Therefore, it was speculated that  $\beta$ -elemene suppressed RNV specifically by downregulating VEGF expression. This was also supported by the observation that  $\beta$ -elemene did not influence the protein expression of other angiogenic factors in mice retinas, including PD-ECGF, TGF and TNF.

Studies focusing on the effects of  $\beta$ -elemene on VEGF are extremely uncommon, with only one report demonstrating that  $\beta$ -elemene inhibits melanoma growth and metastasis via VEGF suppression, but they did not explore the mechanism (9). The present study aimed to explore the mechanisms underlying the inhibitory effects of  $\beta$ -elemene on VEGF expression and RNV. The study's focus was on miRNAs, which are small, single stranded, non-coding RNAs that regulate gene expression by directly degrading mRNA or suppressing post-transcriptional protein translation by binding to the 3'-UTR of their target mRNAs (28). It has previously been shown that miR-218 and miR-410 inhibit oxygen-induced RNV (14,29).

Therefore, microRNA microarrays were used to screen out differentially expressed miRNAs in the normoxia, OIR and OIR-treated groups. The results demonstrated that miR-22, miR-181a-1, miR-335-5p, miR-669n, miR-190b, miR-27a, and miR-93 were upregulated in the OIR-treated group and downregulated in the OIR group, compared with the control. The potential target genes of miR-27a were identified with TargetScan and miRanda. The 3'-UTR of VEGF was found to contain one potential miR-27a binding site. Luciferase assays were used to test whether miR-27a could directly bind to VEGF. The results showed that VEGF was a target gene of miR-27a. In addition, overexpression of miR-27a decreased the expression of VEGF, and  $\beta$ -elemene upregulated miR-27a expression *in vivo* and *in vitro*. Furthermore, when miR-27a expression was reduced by miR-27a inhibitor, the protective effect of  $\beta$ -elemene on RNV was eliminated. Thus, it was hypothesized that  $\beta$ -elemene reduced RNV via miR-27a regulation.

Taken together, it was concluded that  $\beta$ -elemene inhibited RNV in OIR mouse models by reducing VEGF expression via miR-27a. This novel finding may encourage further investigation of the therapeutic role of  $\beta$ -elemene in the pathogenesis of these diseases. The exact mechanisms underlying the regulation of miR-27a expression by  $\beta$ -elemene remain unclear, and further experiments are necessary to understand how  $\beta$ -elemene regulates miR-27a.

#### Acknowledgements

Not applicable.

#### Funding

No funding was received.

#### Availability of data and materials

All data generated or analyzed during the present study are included in this published article.

#### Authors' contributions

LC designed the experiments. WZ conducted all experiments and wrote the manuscript. JG, LL and LX analyzed the data and discussed the results. All authors read and approved the final manuscript.

#### Ethics approval and consent to participate

Animal experiments were conducted following the principles of the Animal Experiment Committee of The First Affiliated Hospital of China Medical University, and the study was approved by the ethics committee of The First Affiliated Hospital of China Medical University, Shenyang, China.

#### Patient consent for publication

Not applicable.

#### Competing interests

The authors declare that they have no competing interests.

#### References

1. Yoshida S, Kobayashi Y, Nakao S, Sassa Y, Hisatomi T, Ikeda Y, Oshima Y, Kono T, Ishibashi T and Sonoda KH: Differential association of elevated inflammatory cytokines with postoperative fibrous proliferation and neovascularization after unsuccessful vitrectomy in eyes with proliferative diabetic retinopathy. *Clin Ophthalmol* 11: 1697-1705, 2017.
2. Jiang Y and Mieler WF: Update on the use of anti-VEGF intravitreal therapies for retinal vein occlusions. *Asia Pac J Ophthalmol (Phila)* 6: 546-553, 2017.
3. Fagerholm R and Vesti E: Retinopathy of prematurity-from recognition of risk factors to treatment recommendations. *Duodecim* 133: 337-344, 2017.
4. Wu W, Duan Y, Ma G, Zhou G, Windhol C, D'Amore PA and Lei H: AAV-CRISPR/Cas9-mediated depletion of VEGFR2 blocks angiogenesis *in vitro*. *Invest Ophthalmol Vis Sci* 58: 6082-6090, 2017.
5. Di Y, Nie QZ and Chen XL: Matrix metalloproteinase-9 and vascular endothelial growth factor expression change in experimental retinal neovascularization. *Int J Ophthalmol* 9: 804-808, 2016.
6. Chang Z, Gao M, Zhang W, Song L, Jia Y and Qin Y: Beta-elemene treatment is associated with improved outcomes of patients with esophageal squamous cell carcinoma. *Surg Oncol* 26: 333-337, 2017.
7. Liu Y, Jiang ZY, Zhou YL, Qiu HH, Wang G, Luo Y, Liu JB, Liu XW, Bu WQ, Song J, *et al*:  $\beta$ -elemene regulates endoplasmic reticulum stress to induce the apoptosis of NSCLC cells through PERK/IRE1 $\alpha$ /ATF6 pathway. *Biomed Pharmacother* 93: 490-497, 2017.
8. Wu J, Tang Q, Yang L, Chen Y, Zheng F and Hann SS: Interplay of DNA methyltransferase 1 and EZH2 through inactivation of Stat3 contributes to  $\beta$ -elemene-inhibited growth of nasopharyngeal carcinoma cells. *Sci Rep* 7: 509, 2017.
9. Chen W, Lu Y, Wu J, Gao M, Wang A and Xu B: Beta-elemene inhibits melanoma growth and metastasis via suppressing vascular endothelial growth factor-mediated angiogenesis. *Cancer Chemother Pharmacol* 67: 799-808, 2011.
10. Yan B, Zhou Y, Feng S, Lv C, Xiu L, Zhang Y, Shi J, Li Y, Wei P and Qin Z:  $\beta$ -Elemene-Attenuated tumor angiogenesis by targeting notch-1 in gastric cancer stem-like cells. *Evid Based Complement Alternat Med* 2013: 268468, 2013.
11. Di Y, Zhang Y, Yang H, Wang A and Chen X: The mechanism of CCN1-enhanced retinal neovascularization in oxygen-induced retinopathy through PI3K/Akt-VEGF signaling pathway. *Drug Des Devel Ther* 9: 2463-2473, 2015.
12. Sui A, Zhong Y, Demetriades AM, Lu Q, Cai Y, Gao Y, Zhu Y, Shen X and Xie B: Inhibition of integrin  $\alpha$ 5 $\beta$ 1 ameliorates VEGF-induced retinal neovascularization and leakage by suppressing NLRP3 inflammasome signaling in a mouse model. *Graefes Arch Clin Exp Ophthalmol* 256: 951-961, 2018.

13. Liu WL: MicroRNA-9 inhibits retinal neovascularization in rats with diabetic retinopathy by targeting vascular endothelial growth factor A. *J Cell Biochem*: Nov 28, 2018 (Epub ahead of print) doi: 10.1002/jcb.28081.
14. Chen N, Wang J, Hu Y, Cui B, Li W, Xu G, Liu L and Liu S: MicroRNA-410 reduces the expression of vascular endothelial growth factor and inhibits oxygen-induced retinal neovascularization. *PLoS One* 9: e95665, 2014.
15. Ye EA and Steinle JJ: miR-146a suppresses STAT3/VEGF pathways and reduces apoptosis through IL-6 signaling in primary human retinal microvascular endothelial cells in high glucose conditions. *Vision Res* 139: 15-22, 2017.
16. Smith LE, Wesolowski E, McLellan A, Kostyk SK, D'Amato R, Sullivan R and D'Amore PA: Oxygen-induced retinopathy in the mouse. *Invest Ophthalmol Vis Sci* 35: 101-111, 1994.
17. Chikaraishi Y, Shimazawa M and Hara H: New quantitative analysis, using high-resolution images, of oxygen-induced retinal neovascularization mice. *Exp Eye Res* 84: 529-536, 2007.
18. Park K, Chen Y, Hu Y, Mayo AS, Kompella UB, Longeras R and Ma JX: Nanoparticle-mediated expression of an angiogenic inhibitor ameliorates ischemia-induced retinal neovascularization and diabetes-induced retinal vascular leakage. *Diabetes* 58: 1902-1913, 2009.
19. Yuan LH, Chen XL, Di Y and Liu ML: CCR7/p-ERK1/2/VEGF signaling promotes retinal neovascularization in a mouse model of oxygen-induced retinopathy. *Int J Ophthalmol* 10: 862-869, 2017.
20. Livak KJ and Schmittgen TD: Analysis of relative gene expression data using real-time quantitative PCR and the 2(-Delta Delta C(T)) method. *Methods* 25: 402-408, 2001.
21. Thomsen R, Sølvsten CA, Linnet TE, Blechinger J and Nielsen AL: Analysis of qPCR data by converting exponentially related Ct values into linearly related X0 values. *J Bioinform Comput Biol* 8: 885-900, 2010.
22. Jiang N, Chen XL, Yang HW and Ma YR: Effects of nuclear factor  $\kappa$ B expression on retinal neovascularization and apoptosis in a diabetic retinopathy rat model. *Int J Ophthalmol* 8: 448-452, 2015.
23. Nicholson L, Vazquez-Alfageme C, Patrao NV, Triantafyllopoulou I, Bainbridge JW, Hykin PG and Sivaprasad S: Retinal nonperfusion in the posterior pole is associated with increased risk of neovascularization in central retinal vein occlusion. *Am J Ophthalmol* 182: 118-125, 2017.
24. Cabral T, Mello LGM, Lima LH, Polido J, Regatieri CV, Belfort R Jr and Mahajan VB: Retinal and choroidal angiogenesis: A review of new targets. *Int J Retina Vitreous* 3: 31, 2017.
25. Mi XS, Yuan TF, Ding Y, Zhong JX and So XF: Choosing preclinical study models of diabetic retinopathy: Key problems for consideration. *Drug Des Devel Ther* 8: 2311-2319, 2014.
26. Sato T, Kusaka S, Shimojo H and Fujikado T: Vitreous levels of erythropoietin and vascular endothelial growth factor in eyes with retinopathy of prematurity. *Ophthalmology* 116: 1599-1603, 2009.
27. Hu J, Hoang QV, Chau FY, Blair MP and Lim JI: Intravitreal anti-vascular endothelial growth factor for choroidal neovascularization in ocular histoplasmosis. *Retin CASES Brief* 8: 24-29, 2014.
28. Falcone G, Felsani A and D'Agnano I: Signaling by exosomal microRNAs in cancer. *J Exp Clin Cancer Res* 34: 32, 2015.
29. Han S, Kong YC, Sun B, Han QH, Chen Y and Wang YC: microRNA-218 inhibits oxygen-induced retinal neovascularization via reducing the expression of roundabout 1. *Chin Med J (Engl)* 129: 709-715, 2016.